IOSR Journal of Applied Chemistry (IOSR-JAC)
e-ISSN: 2278-5736.Volume 13, Issue 5 Ser. III (May. 2020), PP 54-66
www.iosrjournals.org

Effect of dissolved organic matter, DOM on the kinetics of simultaneous studies of oxidation of arsenic(III) and reduction of chromium(VI) in aqueous phase.

Iorhuna, T. Boniface[1], Wuana, A. Raymond[2] and Yiase, G. Stephen[3], Azuaga I. Chia[1] and Myina M. Othniel[1].

[1](Department of Chemistry, Faculty of Science, Taraba State University Jalingo, Nigeria)
[2](Department of Chemistry, College of science, University of Agriculture Makurdi, Nigeria)
[3](Department of Chemistry, Faculty of Science, Benue State University Makurdi, Nigeria).

Abstract:
A kinetic approach was used to study the oxidation of As(III) and reduction of Cr(VI) simultaneously in aqueous phase, and in the presence of DOM. Reactions were monitored by UV-visible spectrophotometry. The stoichiometry of the reaction was 1 : 3 ($Cr_2O_7^{2-}$ to AsO_2^-). The reaction products were identified as Cr(III) and As(V). DOM was characterized by UV-visible Spectrophotometry, Fourier Transform Infrared Spectroscopy, FTIR and Scanning Electron Microscopy, SEM. The rate equation for the reaction is proposed as
$-d[Cr_2O_7^{2-}]/dt = k_2[Cr_2O_7^{2-}][AsO_2^-]$
where k_2 is the second order rate constant. The reaction rate increased with increase in the volumes of DOM. The rate depended on pH and independent of the ionic strength when DOM was added. The activation energy, E_a were 52.01 kJmol^{-1}, 48.22 kJmol^{-1} and 46.46 kJmol^{-1} for $AsO_2^-/Cr_2O_7^{2-}$, $AsO_2^-/Cr_2O_7^{2-}$/Saw Dust and $AsO_2^-/Cr_2O_7^{2-}$/Maize Cob couples respectively, enthalpy change, ΔH, were more negative (-49.54 kJmol^{-1}) for $AsO_2^-/Cr_2O_7^{2-}$ couple than others, and entropy change, $+\Delta S$ were most negative (-132.20 Jmol^{-1}K^{-1}) for $AsO_2^-/Cr_2O_7^{2-}$/Maize Cob and less negative for the other couples.

Key Words; *Arsenic(III), chromium(VI), kinetics, oxidation-reduction, dissolved organic matter*

Date of Submission: 01-06-2020 Date of Acceptance: 16-06-2020

I. Introduction

As human needs increase and civilization changes, more and more finished products of different types are required. Accordingly, large number of industries process waste streams that get in to the environment and may contain potentially toxic metals at concentrations above the acceptable limits [1]. Environmental contamination can also occur through metal corrosion, atmospheric deposition, soil erosion of metal ions and leaching of heavy metals, sediment re-suspension and metal evaporation from water resources to soil and ground water. Natural phenomena such as weathering and volcanic eruptions have also been reported to significantly contribute to heavy metal pollution [2]. Industrial sources include metal processing in refineries (mining operations), coal burning in power plants, petroleum combustion, electronic device manufacturing units, nuclear power stations and high tension lines, metal-plating facilities, plastics, textiles, tanneries, microelectronics, wood preservation and paper processing plants [3]. The waste streams from the plants contain toxic heavy metals and are not easily removed without specialized or advanced treatment [1].

Among the priority metals that are of great public health significance are arsenic and chromium which are toxic to humans and animals. Chromium is released into the environment by various industries including electro-plating, chromate manufacturing, leather tanning and wood preservation. In the environment, Chromium exists primarily as Cr(VI) and Cr(III), with Cr(VI) being of significant concern due to its carcinogenicity [4]. Arsenic is ubiquitous in the earth's crust, and elevated arsenic in the environment is primarily attributed to anthropogenic sources, including industrial waste products, agricultural pesticides and wood preservatives. The predominant inorganic forms of arsenic in the environment are As(V) and As(III). As(V) is mainly present in the environment as $H_2AsO_4^-$ and $HAsO_4^{2-}$ as most soluble forms and most likely partially as H_3AsO_4 or AsO_4^{3-}, while As(III) dominates in sediments as H_3AsO_3 at pH below 9.2 [5]. As(III) is more toxic and mobile than As(V) in the environment. In Schimatari's's water supply for instance, As concentrations up to 34 μgL^{-1} along with Cr(VI) levels up to 40 μgL^{-1} were detected. In the Asopos River, total chromium values were up to 13 μgL^{-1}, hexavalent chromium was less than 5 μgL^{-1} and other toxic elements were relatively low [6]. Therefore, Cr(VI) reduction and As(III) oxidation are desirable to reduce their adverse impact on the environment [7].

Also, various agricultural and industrial wastes are found to lethal the environment, especially within the areas in which such wastes are produced. Saw dusts and Maize cob which are produced at one point or the other in Nigeria and have been found to be of little or no use, if converted in to biochar, can be used to produce dissolved organic matter, DOM. The effect of the organic matter obtained from these wastes on the oxidation of arsenic(III) and reduction of chromium(VI) may turn out to be a greener approach to the remediation of these heavy metals.

II. Materials And Methods

2.1 Chemicals, Reagents and Apparatus

$K_2Cr_2O_7$ (JHD^{AR}), CrO_3 (LOBA^{AR} CHEMIE PVT Ltd), Cr_2O_3 (LOBA^{AR} CHEMIE PVT Ltd), $NaAsO_2$ (LOBA^{AR} CHEMIE PVT Ltd), HNO_3 (BDH^{AR}), $NaNO_3$ (Fenxichun^{AR}), $FeCl_3$ (LOBA^{AR} CHEMIE PVT Ltd), saw dust, maize cob, H_2SO_4 (97 – 99 % assay, JHD^{AR}), O-phosphoric acid, (Fenxichun^{AR}), o-phenanthroline (Qualikems^{AR}), $FeSO_4.7H_2O$ (JHD^{AR}), $Fe(NH_4)_2(SO_4)_2.6H_2O$ (LOBA^{AR} CHEMIE PVT Ltd), acrylamide (JHD^{AR}), methanol (99.9 % Fisher Chemical^{AR}), distilled and deionised water, muffle furnace (NEY M-525), mechanical shaker (HY-2 Speed adjusting multipurpose vibrator), thermostatic water bath (Clifton unstirred bath model 92498), UV-visible spectrophotometer (Unico^{R} 2800P), pH meter (Hanna Instrument H19024), analytical balance (aeADAM PW 184, AE 437531), freeze dryer (Lyodry, Grande freeze dryer model), FTIR spectrophotometer (Agilant Technolologies, Cary 630 FTIR), Sieve (Cole Parmer-typed sieve of 0.80 mm mesh) and normal laboratory glasswares.

2.2 Determination of UV-visible Spectrum of the Cr(VI) and Cr(III)

Solutions of the salts of CrO_3 and Cr_2O_3 were prepared (with 0.009 $molL^{-1}$) and the absorbances of the solutions taken in the wavelength range (300-750 nm) with a Unico^{R} 2800P UV-visible spectrophotometer [8]. The wavelengths of maximum absorption were obtained by plot of absorbances versus wavelengths.

2.3 Preparation and Characterization of DOM from Sawdust, SD and Maize Cob, MC

The waste materials were collected locally; sawdust from a local sawmill (along George Akume Road, International Market, Makurdi, Benue State-Nigeria) and corn cob waste from a maize farm (at Jauro Yinu, Wukari Road, Jalingo, Taraba State-Nigeria). The saw dust was sieved with a Cole Parmer-typed sieve of about 0.80 mm mesh in order to obtain a desirable size fraction. Then, the sieved saw dust was washed with distilled water to remove any residues or impurities such as ash and dust. Corn cob on the other hand were first washed with distil water, dried in an oven and grounded through the sieve to lower the surface area, followed by the procedure described above [9, 10].

Subsequently, these were dried in an oven. After drying, the materials were pyrolysized (at < 350 ^{o}C) in a furnace to obtain the biochar [9].

A sample of the biochar obtained from saw dust and maize cob each were suspended in a reaction vessel with deionized water, and agitated on a shaker at an average speed at room temperature for 24 hours (to reach an apparent equilibrium). The suspensions were then passed through a filter paper and then a 0.2 µm membrane filter to obtain dissolve organic matter, (DOM) [7]. The percentage mass/volume of DOM was analyzed by Walkley-Black titrimetric method [10 - 12].

In determining the chemical structure and functional groups involved in As and Cr redox reactions, DOM samples (DOM(SD) and DOM(MC) containing a percentage weight by volume of carbon were analyzed. To achieve this, 300 mL of DOM samples each containing varying percentage by volume DOM (plus 300 mL of DOM that took part in the reaction) were freeze-dried and analyzed. The functional groups were analyzed after freeze drying the DOM samples using FTIR and UV-visible spectrophotometers. The colours of the solutions used were also observed to see the changes that occur, the nature of DOM surfaces were also observed before and after taking part in the redox reactions using scanning electron microscopy, SEM [7, 13].

2.4 Stoichiometric Studies

The Stoichiometry of the reaction was determined by UV-visible spectrophotometric titration. Here, reaction mixtures containing fixed volume 10.00 mL (6.0×10^{-5} $molL^{-1}$) of As(III) and varying volumes 2, 4, 6, 8 and 10 mL (concentrations; 1.0×10^{-3} to 1.4×10^{-2} $molL^{-1}$) of Cr(VI) at constant I of 0.1 $molL^{-1}$ ($NaNO_3$), T = ambient (297 – 300 K) and pH = 6 were allowed to go to completion. The absorbances of the solutions were taken at the wavelength of maximum absorbance of the Cr(VI) metal salt. The equivalent point was obtained from the plots of absorbances of the solutions against their concentrations [14].

2.5 Kinetic Studies

All rate measurements were made using Unico^{R} 2800P UV-visible spectrophotometers at the wavelengths of maximum absorptions. The reaction rates were monitored at the wavelength by noting the

decrease in absorbances of the reaction mixtures with time. The results were interpreted based on the fact that, Beer's law is additive for a multi component sample, equations 1 and 2

$$(A)\lambda_1 = (\varepsilon_{Cr(VI)})\lambda_1 l C_{Cr(VI)} + (\varepsilon_{Cr(III)})\lambda_1 l C_{Cr(III)} \quad (1)$$

$$(A)\lambda_2 = (\varepsilon_{Cr(VI)})\lambda_2 l C_{Cr(VI)} + (\varepsilon_{Cr(III)})\lambda_2 l C_{Cr(III)} \quad (2)$$

where A is the absorbances of the mixtures, λ_1 and λ_2 are wavelengths at which the absorbances were measured, $\varepsilon_{Cr(VI)}$ and $\varepsilon_{Cr(III)}$ are the molar absorptivities, $C_{Cr(VI)}$ and $C_{Cr(III)}$ are the concentrations and l is the path length [15].

All kinetic measurements were made under pseudo-first order conditions with the concentrations of AsO_2^- at least 60 times greater than that of the $Cr_2O_7^{2-}$ or $Cr_2O_7^{2-}$ at least 60 times greater than that of the AsO_2^- [8].

The pseudo-first order rate constants, k_{obs}, were obtained from the plots of $\ln(A_t\text{-}A_\infty/A_o\text{-}A_\infty)$ against time (where A_t, A_o and A_∞ are the absorbances of the reaction mixtures at times t, zero time and infinite time respectively). Plots of $\log k_{obs}$ vs. $\log[AsO_2^-]$ and $\log k_{obs}$ vs. $\log[Cr_2O_7^{2-}]$ have been determined, with $[AsO_2^-]$ = 2.00, 4.00, 6.00, 8.00 and 10.00 (x 10^{-2} molL^{-1}) and $[Cr_2O_7^{2-}]$ = 2.00, 4.00, 6.00, 8.00 and 10.00 (x 10^{-2} molL^{-1}). The temperature was kept constant at ambient (297 – 300 K), pH = 6 and I = 0.1 molL^{-1}.

2.6 pH Dependence Studies

The pseudo first order rate constants, k_{pH} for the oxidation-reduction reaction involving As(III)/Cr(VI) and DOM/As(III)/Cr(VI) reactions were determined at pH in the range of 2 – 10 (using HNO_3 and NaOH) while keeping other conditions constant.

2.7 Temperature Dependence Studies

The temperature dependence rate study for the oxidation-reduction reaction involving As(III)/Cr(VI) and DOM/As(III)/Cr(VI) reactions were carried out over the temperature range of 288 K - 305 K and 273 K while keeping other conditions constant. Kinetic activation parameters (activation energy, E_a, entropy change, ΔS, and enthalpy change, ΔH) were obtained from Arrhenius and Eyring plots [16 - 18].

2.8 Ionic Strength Effect

The effect of ionic strength changes on rate of the oxidation-reduction reaction involving As(III)/Cr(VI) and DOM/As(III)/Cr(VI) reactions have been studied over the range of (0.001 - 0.021) molL^{-1} concentrations of $NaNO_3$ salt while keeping other conditions constant.

III. Results And Discussion

3.1 Spectra consideration of the solutions used

In Figure 1 above and Table 1, the bands correspond to the d – d transitions; the redistribution of electrons among orbitals that are mainly localized on the metal atoms or charge-transfer (CT) transitions involving the metal d-orbitals. Typically, the bands above 300 nm and below 850 nm, involve the motion of electrons from an essentially ligand-based orbital to an essentially metal-based, or vice versa. This makes charge to be transferred from one atom to another. In general, it is referred to as ligand – to – metal charge – transfer (LMCT). CT bands are observed if the energies of empty and filled ligand- and metal-centered orbitals are similar. It occurs within the visible or near UV region of the spectrum [8, 15]. Thus the kinetic studies were done using UV-visible spectrophotometry and at the established wavelengths of maximum absorbances of the solutions used.

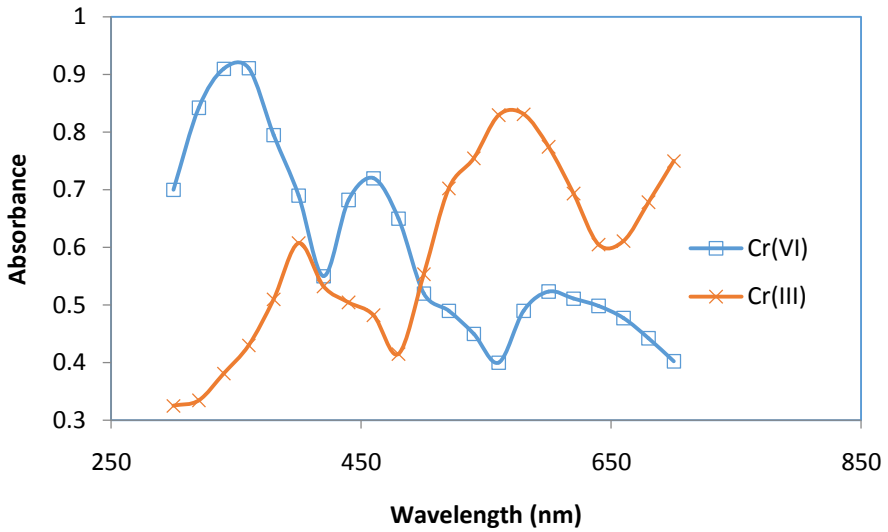

Figure 1: Determination of λ_{max} for Cr(VI) and Cr(III) ions

3.2 Reaction Stoichiometry

The calculation of the concentrations at the equivalence point of the UV-visible spectrophotometric titration (as shown in Figure 2) gave the stoichiometry of the reaction as 1: 3 ($Cr_2O_7^{2-}$: AsO_2^-). Similar stoichiometry has been reported for the reaction between paracetamol and dichromate ion [14, 19].

$$Cr_2O_7^{2-} + 3C_8H_9NO_2 + 8H^+ \rightarrow 2Cr^{3+} + 3C_8H_7NO_2 + 7H_2O \quad (3)$$

The equation for the reaction between $Cr_2O_7^{2-}$ and AsO_2^- ions can be given as;

$$Cr_2O_7^{2-} + 3AsO_2^- + 8H^+ \rightarrow 2Cr^{3+} + 3AsO_3^- + 4H_2O \quad (4)$$

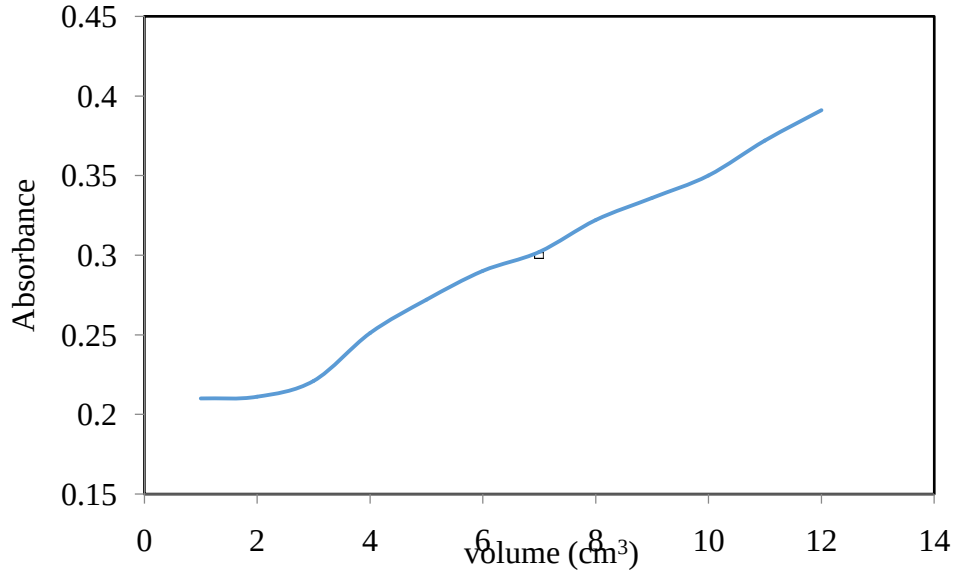

Figure 2: UV-visible spectrophotometric titration for the reaction between AsO_2^- and $Cr_2O_7^{2-}$

3.3 Characterization of the Dissolved Organic Matter, DOM samples

3.3.1 UV-visible/FTIR studies

The DOM samples were characterised by measuring the content of their humic materials. In achieving this, 300 mL each from the DOM samples were freeze dried using a freeze drier, after which the DOM samples were characterised by UV-visible and FTIR spectrophotometers [7, 13].

UV-visible and FTIR spectroscopy are powerful tools that can be used in the identification of complex (organic) compounds. These enable chemists to obtain absorption spectral of compounds that are a unique reflection of their molecular structures (including bands of humic materials) [20].

From the UV-visible spectral of these DOM samples (Figure 3), it can be seen that the wavelength of maximum absorption were found as 250 nm DOM(SD) and 260 nm DOM(MC). In both cases the UV-visible spectral have

shown similarities in the peaks, which is in agreement with other studies [21]. The UV-visible spectral data of the DOM samples were recorded in ethanol in the wavelength range 200 - 600 nm at ambient temperature (298 – 300 K), using a 1.0 cm quartz cell, reference was pure water. Samples were diluted to maintain the maximal response [21].

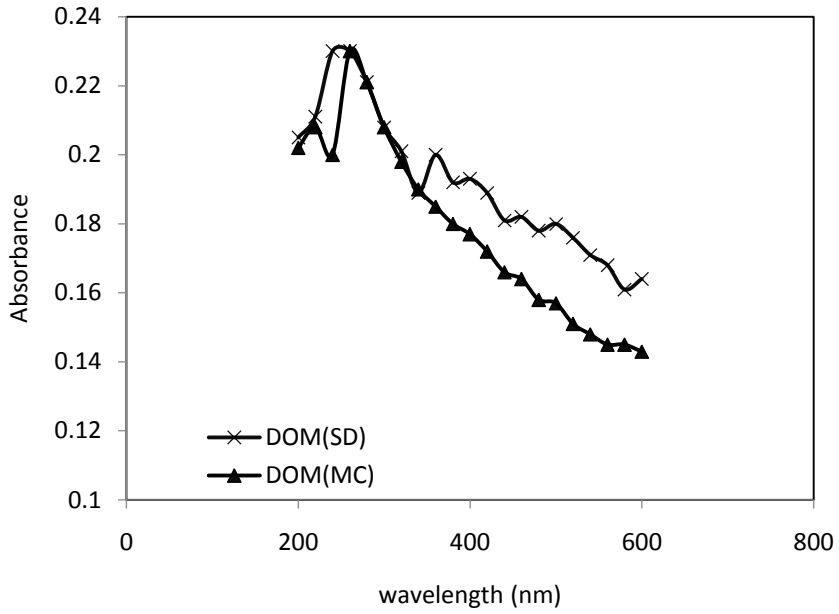

Figure 3: Determination of λ_{max} for the dissolved organic matter, DOM from saw dust, SD and maize cob, MC

The characteristic energy of a transition and the wavelength of radiations absorbed are properties of a group of atoms rather than of electrons themselves. The group of atoms producing such absorption is called a chromophore [22]. The electronic spectral data of humic materials have λ_{max} at 254 nm [23]. These UV-visible spectral data from the DOM samples might have been contributed by phenolic, aromatic carboxylic, and polycyclic aromatic compounds of the humins [21]. The bands may be attributed to $\pi \rightarrow \pi^*$ and n $\rightarrow \pi^*$ transitions [21 and 23].

The IR spectral of both DOM samples have been obtained (Figures 4a and 4b), (Table 1 has the spectral data for these bands). They have a variety of bands typical of those for humic materials (humic and fulvic acids). The major absorption bands are found in the regions of 2500 – 3500 cm^{-1} and 650 - 770 cm^{-1} (O-H stretching and out of plane bending groups), 2500 – 3500 cm^{-1}, 1350 – 1470 cm^{-1} and 690 – 900 cm^{-1} (C–H stretching, deformation, and bending and ring puckering respectively), 1650 – 1800 cm^{-1} (C=O stretching of COOH), 1620 – 1680 cm^{-1} (alkene/aromatic C=C stretching), 970 – 1250 cm^{-1} (C–O stretching of alcohols/phenols) 880–995 cm^{-1} and 1395 – 1440 cm^{-1} (=C–H out of plane bending/C-O-H bending). These spectra evidently show predominance of OH and COOH groups which are the most characteristic features of humic materials. It is obvious that the IR results are in good agreement with the other characterization findings [20 - 23].

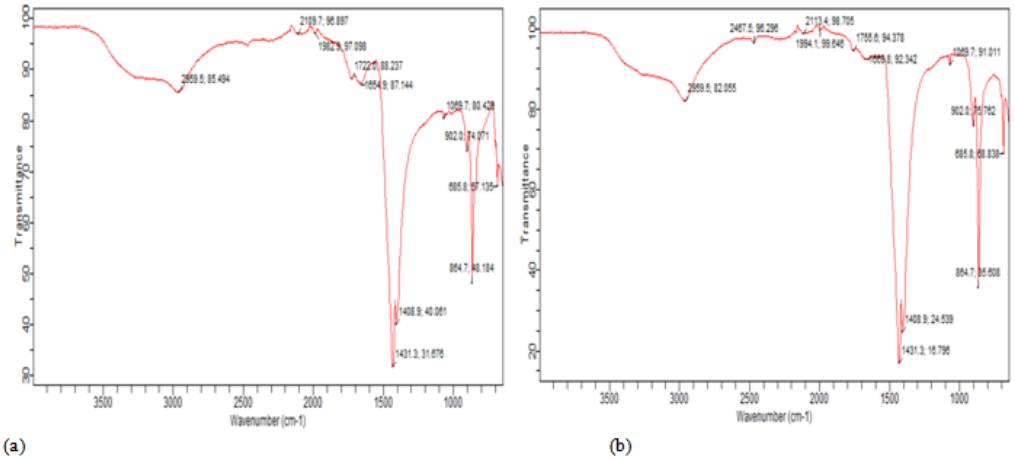

Figure 4: Infra-red spectral of the dissolved organic matter, DOM obtained from (a) saw dust and (b) maize cob

Table 1: UV-visible and Infra-red spectral data of the dissolved organic matter, DOM from saw dust and maize cob

λ_{max} (nm)/ Infra-red frequencies (cm^{-1})	Dissolved organic matter	
	Saw dust	Maize cob
λ_{max}	250.00	260.00
$\upsilon_{(O-H)}$ (COOH)	2959.5	2959.5
$\upsilon_{(C-H)}$ (SP^3)	2959.5	2959.5
$\upsilon_{(C=O)}$	1755.6	1722.0
$\upsilon_{(C=C)}$	-	1654.9
$\upsilon_{(-C-O-)}$ (alcohol/phenols)	1069.7	1069.7
$\upsilon_{(\mathbf{CH_2}\ \&\ \mathbf{CH_3})}$	1408.9	1408.9
$\upsilon_{(=C-H)}$	902.0	902.0
$\upsilon_{(C-H)}$ (arene)	864.7	864.7
$\upsilon_{(O-H)}$ (phenol/alcohols)	685.8	685.8
$\upsilon_{(C-O-H)}$	1431.3	1431.3

3.3.2 SEM studies

Figures 5 and 6, showed the scanning electron microscopies, SEMs which were used to study the physical morphology of the dissolved organic matter before and after reacting with the redox reactants {As(III)/Cr(VI)}. A careful observation of the morphologies of these DOM samples has shown the nature of the micrographs before reaction and after taking part in the redox reactions. These can be seen to change in their surfaces after the DOM samples took part in the reactions [7].

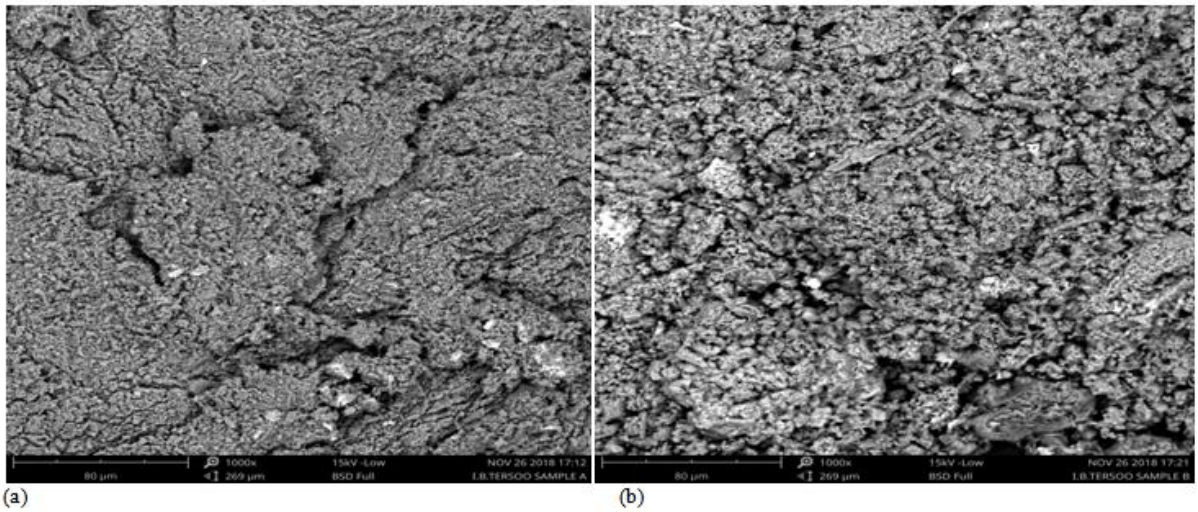

(a) (b)

Figure 5: Scanning electron microscopy, SEM of the dissolved organic matter, DOM obtained from (a) saw dust and (b) maize cob

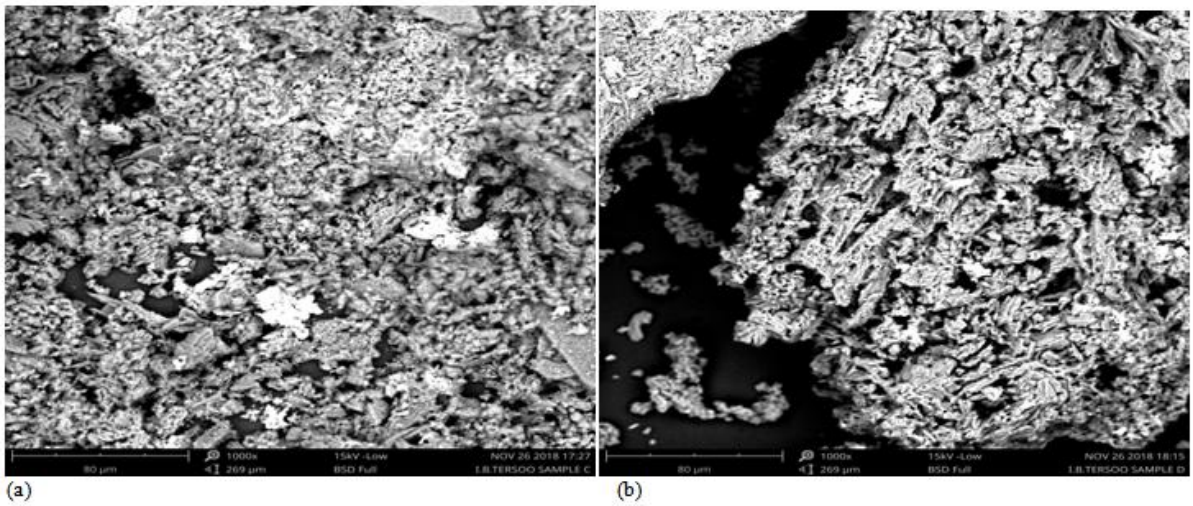

(a) (b)

Figure 6: Scanning electron microscopy, SEM of the DOM obtained from (a) saw dust, (b) maize cob that took part in the redox reaction.

On the basis of the UV-visible spectrophotometric, infra-red spectrophotometric and scanning electron microscopy analysis, it can be said that, those samples (obtained from saw dust, SD and maize cob) contained DOM that also evidently reduced Cr(VI) to Cr(III) {as the colour changed from yellow Cr(VI) to green Cr(III)}, as well as the changes that occur in the DOM surfaces as seen in the SEM results. Also, the similarity of these absorption bands indicated that many similar structural and functional groups existed in the DOM from the various agro wastes.

3.4 Effect of the Initial Concentration on the Reaction Rate

In considering the effects of the concentration on the reactions rate, varying amounts of AsO_2^- ions (0.02, 0.04, 0.06, 0.08 and 0.10 molL^{-1}) were used against a fixed $Cr_2O_7^{2-}$ ions (0.009 molL^{-1}) concentration and fixed amounts of $Cr_2O_7^{2-}$ (0.008 molL^{-1}) with AsO_2^- (0.009 molL^{-1}) were used against varying weight/volume percentages of DOM (10, 20, 30, 40 and 50 mL). These reactions were monitored using JENWAY 7315 UV-visible spectrophotometers at ambient temperature (298 – 300 K), ionic strength of 0.1 molL^{-1} $NaNO_3$, pH of 6 and time intervals of 15, 30, 45, 60 and 75 seconds for each amount of the substance. Pseudo-first order plots of $\ln[A_t–A_\infty/A_0\text{-}A_\infty]$ versus time were made from the reactions involving AsO_2^- ion and $Cr_2O_7^{2-}$ ion. From these plots; the oxidation-reduction reactions (of AsO_2^- with $Cr_2O_7^{2-}$) are linear to more than 70% extent of the reactions. The linearity of the plots suggests that the reaction is first order in both AsO_2^- and $Cr_2O_7^{2-}$ ions. Table 2 contains the values of k_{obs} for the oxidation-reduction reaction involving AsO_2^- and $Cr_2O_7^{2-}$ ions and the results show an increase in k_{obs} values with increase in concentration in both cases. Also, plots of logk_{obs} versus log$[AsO_2^-]$ and logk_{obs} versus log$[Cr_2O_7^{2-}]$ showed a linear relationship (having regression of 0.989 and 0.957 respectively) with the slopes of approximately 1.00; implying that the reaction is first order in both AsO_2^- and $Cr_2O_7^{2-}$ ions. Hence, the reaction is second order overall, which is in agreement with other works [8, 19]. Therefore the rate equation for the reaction is as follows

$$-\frac{d[Cr_2O_7^{2-}]}{dt} = k_2[Cr_2O_7^{2-}][AsO_2^-] \quad (5)$$

The results of oxidation-reduction reactions of AsO_2^- and $Cr_2O_7^{2-}$ showed rapid rates with the reactions completing almost before the 75 seconds maximum time for the study and the reactions increased with increase in both AsO_2^- and $Cr_2O_7^{2-}$ ions concentrations. These reactions (or observations) are possible because of the wide variation in the electrode potential of the ions (redox couple) involved; $Cr_2O_7^{2-}$/Cr(III) (+1.38 V) and AsO_2^-/As(V) (-0.56 V) [24, 25]. Also, the reactions rates increase with increase in the concentrations of both $Cr_2O_7^{2-}$ and AsO_2^- as most reactions are faster at higher concentrations because of the resulting more effective collisions from the molecular collisions of the molecules in solution with one another [26].

From Table 2 it can be seen that, the k_{obs} values are higher at varying $Cr_2O_7^{2-}$ ion concentrations than for AsO_2^- ion concentrations. This may be because of the higher electrode potential of $Cr_2O_7^{2-}$ ion over AsO_2^- ion or because of the fact that the pH at which the studies were conducted favoured the $Cr_2O_7^{2-}$ over AsO_2^-. Because, $Cr_2O_7^{2-}$/Cr(III) redox couple has (+1.38 V) and AsO_2^-/As(V) redox couple has (-0.56 V) [24, 25]. Again, the reactions were conducted at pH = 6 (about the pH of natural waters) and the concentrations of these ions are pH dependence as $Cr_2O_7^{2-}$ ion is more in solution as $HCrO_4^-$ ion at this pH and strongly oxidizing. Thus at such pHs the concentration of $HCrO_4^-$ was high coupled with high electrode potential (Figure 10) made the k_{obs} values at varying $Cr_2O_7^{2-}$ concentrations to be higher than those of the AsO_2^- [25 - 28]. Moreover, AsO_2^- dominates as $H_2AsO_3^-$ at alkaline pHs with low electrode potential which might lead to low reaction rates (k_{obs} values), as we react it with $Cr_2O_7^{2-}$ ions at slightly acidic solutions (pH = 6) [24 and 25].

Table 2: Pseudo-first order rate constants, k_{obs} rate data for the oxidation-reduction reaction between AsO_2^- and $Cr_2O_7^{2-}$

$[AsO_2^-]/[Cr_2O_7^{2-}]$ mol L^{-1}	I mol L^{-1}	$k_{obs}/10^2$ (s^{-1}) at varying $[AsO_2^-]$	$k_{obs}/10^2$ (s^{-1}) at varying $[Cr_2O_7^{2-}]$
0.10	0.10	22.00	24.00
0.08	0.10	16.00	17.00
0.06	0.10	12.00	13.00
0.04	0.10	9.00	11.00
0.02	0.10	5.00	7.00

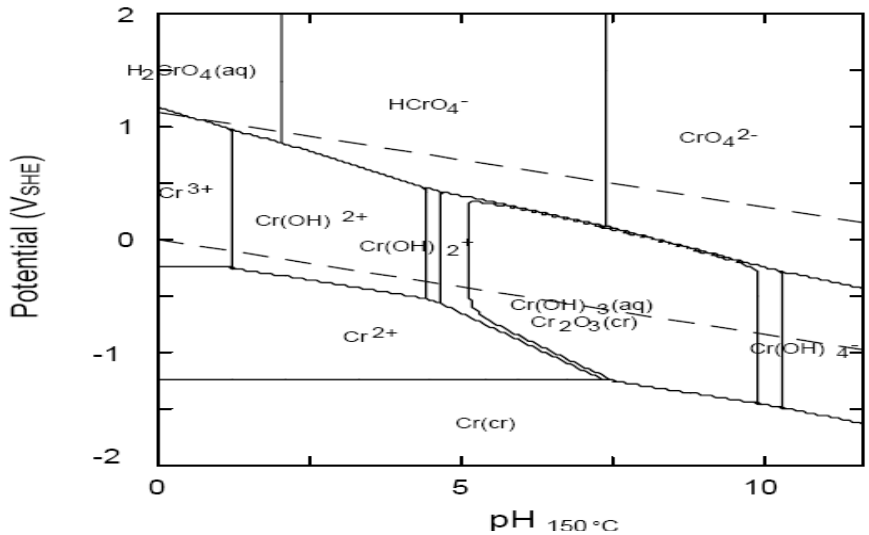

Figure 7: A simplified Pourbaix diagram for Cr species at 150 °C and $[Cr(aq)]_{tot}=10^{-8}$ [26].

3.5 Effect of Dissolved Organic Matter, DOM on the Reactions Rate

Wood sawdust and corn cob have been used as a source of biochar and/or organic matter, which have been seen to reduce Cr(VI) to Cr(III) [7]. After the agro waste materials were pyrolysized (at <350 ^{o}C or 623 K) in a furnace to obtain the biochar [9]. Eight (8) g of the biochar obtained from saw dust and maize cob each were suspended in a 1 L reaction vessel with deionized water, and agitated on a shaker at an average speed, at ambient temperature (288 – 300 K) for 24 hours (to reach an apparent equilibrium). The suspension was then passed through a filter paper and then a 0.2 µm membrane filter where the dissolve organic matter, (DOM) was obtained as filtrate [7]. The amount of DOM in the filtrate was analyzed by Walkley-Black titrimetric method [10 and 11], and was found to contain approximately 0.2738 % DOM from maize cob and 0.2933 % DOM from saw dust. The percentage weight/volume of the DOM from saw dust was higher than that from maize cob. These seem to agree with the percentage lingnocellulosic fibrous material content of these agro waste substances, as saw dusts was shown to have higher pulp material in it [29].

Considering the oxidation-reduction reaction of AsO_2^- and $Cr_2O_7^{2-}$ ions in the presence of DOM, Figure 8 and Table 3, the pseudo first order rate constants, k_{obs} of these reactions at varying percentages weight/volume of DOM from saw dust and DOM from maize cob were determined. Table 3 showed that, DOM has no effect on the reaction rate at the initial volumes used, but turn to increase the rate as the volumes increased, the k_{obs} values of these reactions in the absence of DOM were found as 0.016 s^{-1} and 0.017 s^{-1} for AsO_2^- and $Cr_2O_7^{2-}$ ions at 0.08 $molL^{-1}$, and was found as 0.018 s^{-1} at the same 0.08 $molL^{-1}$ of the metal ions in the presence of 40 cm^3 DOM from saw dust and maize cob. It is even higher with 50 cm^3. However, the increased rate is higher with DOM from saw dust (Table 3), which may be in line with the higher weight/volume percent of the DOM from saw dust compare with DOM from maize cob.

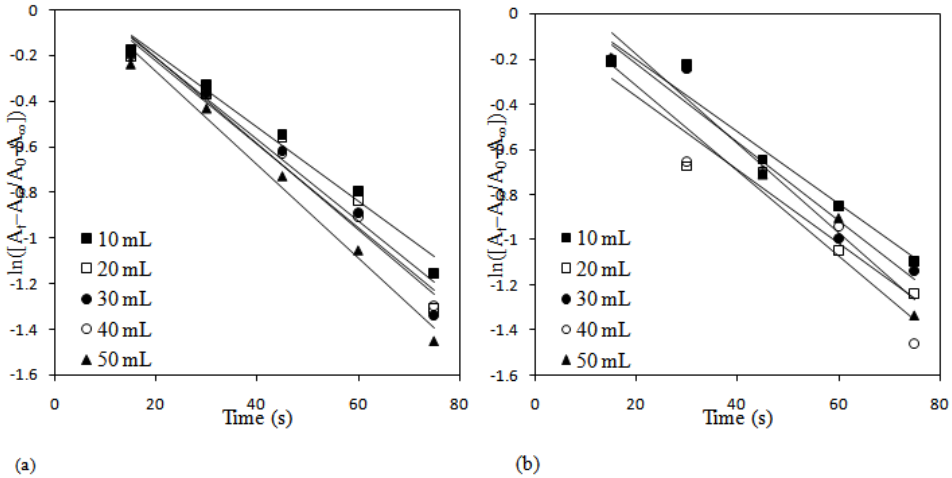

Figure 8: Effects of volumes (mL) of dissolved organic matter, DOM obtained from (a) saw dust and (b) maize cob on the rates of redox reactions between AsO_2^- and $Cr_2O_7^{2-}$.

Table 3: Pseudo-first order rate constants, k_{obs} data for the oxidation-reduction reaction between AsO_2^- and $Cr_2O_7^{2-}$ ions in the presence of dissolved organic matter, DOM.

Volume (mL)	k_{obs}(s^{-1}) for $AsO_2^-/Cr_2O_7^{2-}$/DOM	
	Saw dusts	Maize cob
10	0.016	0.016
20	0.017	0.016
30	0.018	0.017
40	0.018	0.018
50	0.020	0.019

3.6 Effects of pH on the Reaction Rate

Examining the conditions under which the oxidation-reduction reaction of AsO_2^- and $Cr_2O_7^{2-}$ ions may occur in nature is relevant, as these would give good informations on Cr and As speciation in the environment and on the applications of the experimental results that have been obtained. The pH of soil and ground water generally have values between 5 and 9. From Table 4, it can be seen that rate decreases with increase in pH of the acidic range and increases with increase in pH of the alkaline range. Reactions generally increase with concentration, as more reactant molecules mean more effective collisions which give rise to higher proportion of molecules that can overcome the energy barrier to give the products [26]. And the availability of AsO_2^- and $Cr_2O_7^{2-}$ ions in an aqueous environment is dependent on pH, Figure 7 [24 and 25]. That is, Cr(VI) exhibit varying ionic species in solution as the pH changed; the dominant forms include $HCrO_4^-$ at pH 1 - 6 and CrO_4^{2-}at pH >6, other forms are also possible, $HCr_2O_7^-$ and $Cr_2O_7^{2-}$, with their formation requiring Cr(VI) concentration to be greater than 0.1 $molL^{-1}$. On the other hand, AsO_2^- exist in aqueous solution at pH's above 8 and below 13 (with dominance as $H_2AsO_3^-$) especially at low concentrations, and as the pH increases more of the $H_2AsO_3^-$ ions are present in solution giving rise to greater effective collisions which results to more $Cr_2O_7^{2-}$ ions combining (or accepting electrons to become reduced) with AsO_2^- to give the product hence the higher k_{pH} at very basic (8 – 10) pH, [30, 32]. This is however dependent on the nature of the acid used, as HCl results to the formation of chlorochromate ion, CrO_3Cl, while sulphuric acid gives a sulfato complex, $CrO_3(OSO_3)^{2-}$, hence the choice of HNO_3 acid for this research [32]. The ease of reduction of the Cr(VI) species is of the order $HCrO_4^-$ > CrO_4^{2-} > $HCr_2O_7^-$ > $Cr_2O_7^{2-}$, thus the decrease in the reaction rate with increase in pH can be attributable to the presence of $HCrO_4^-$ ions at lower pH, which is more reducing than CrO_4^{2-}. Moreover, the increase in rate constant with increasing [H+] or decrease in pH seems to suggest the protonation of $Cr_2O_7^{2-}$ to give H_2CrO_4 or $HCrO_4^-$ [19, 30 and 31].

Again, Figure 9 has plots of rate of reaction of AsO_2^- and $Cr_2O_7^{2-}$ ions at varying pH in the presence of DOM obtained from saw dust and maize cob. Table 4 contain pseudo-first order rate constant, k_{pH} values of these reactions. The results showed an enhanced rate at lower (acidic) pH in the presence of DOM which may agree with the dominant $HCrO_4^-$ ions over CrO_4^{2-} ions, making them react faster with the AsO_2^- and DOM, and the reaction being monitored with respect to change in the concentration (colour) of Cr(VI) [30 and 31]. Furthermore, at higher pH, there may have been effect of the DOM on the ions, but may not be reasonable enough to be evident on the reaction rate as seen in the k_{obs} values. Also, the major part of humic material (Fulvic acid) which is responsible for oxidation by $Cr_2O_7^{2-}$ ion is soluble over all pH, they have the highest oxygen content than others, have smaller sizes, have many –COOH and C-OH groups, making them more chemically reactive [32 and 33].

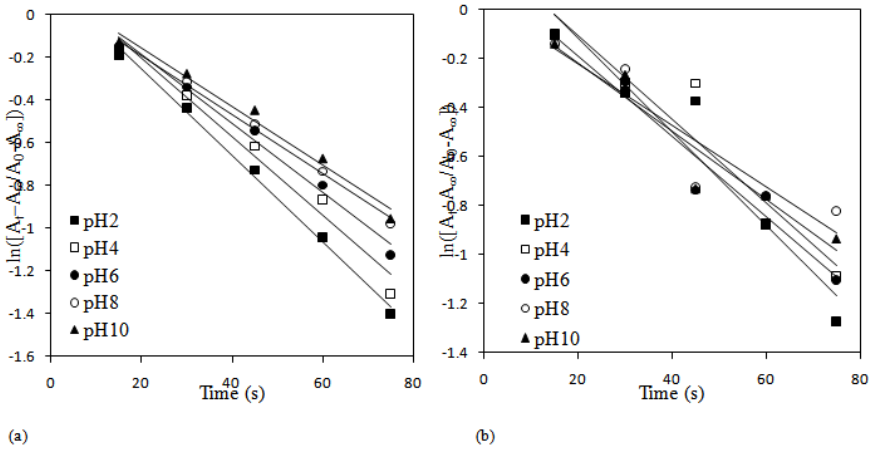

Figure 9: Effects of dissolved organic matter, DOM obtained from (a) saw dust and (b) maize cob on the rates of reaction of AsO_2^- with $Cr_2O_7^{2-}$ at varying pH.

Table 4: Pseudo-first order, k_{pH} data for the oxidation-reduction reaction between AsO_2^- and $Cr_2O_7^{2-}$ and in the presence of dissolved organic matter, DOM from saw dust and maize cob at varying pH.

pH	$k_{pH}(s^{-1})$ for $AsO_2^-/Cr_2O_7^{2-}$	$k_{pH}(s^{-1})$ for $AsO_2^-/Cr_2O_7^{2-}$/DOM	
		Saw dust	Maize cob
2	0.018	0.020	0.019
4	0.016	0.018	0.017
6	0.016	0.016	0.016
8	0.012	0.013	0.012
10	0.013	0.013	0.013

3.7 Effects of Ionic Strength change on the Reaction Rate

Effects of Ionic Strength on the rate of oxidation-reduction reaction between AsO_2^- and $Cr_2O_7^{2-}$ ions were investigated over the range 0.001 – 0.021 molL^{-1} ($NaNO_3$). The results as presented in Table 5 showed that, the reaction rate increase with increase in ionic charge of the solution. This seems to agree with the Kumar, P. 2013 and Hughes-Jones, N. C. et al 1964 in terms of favourable interactions between the reactants and activated complex and the ionic atmosphere of oppositely charged ions which surround them in solution. Here, the charges on AsO_2^- and $Cr_2O_7^{2-}$ ions have the same sign, thus, the activated complex may be more highly charged than the reactants (AsO_2^- and $Cr_2O_7^{2-}$). Increasing the ionic strength of the reaction solution therefore stabilized the activated complex more than the reactants, and thus increase the rate constant by lowering the effective activation energy [34 and 35]. Similarly, effects of ionic strength on the rate of oxidation-reduction reaction between AsO_2^- and $Cr_2O_7^{2-}$ ions in the presence of DOM are presented in Figure 10 for DOM from saw dust and maize cob respectively. It can be seen from Table 5 that, the reaction rate is fairly constant, indicating that the reaction is independent of ionic strength of the solution. Here, a third reactant is included, DOM whose ionic charge is not fully established and this may, in a simple picture, cause no change in the rate constant with change in ionic strength of the reaction as it was observed [34 and 35].

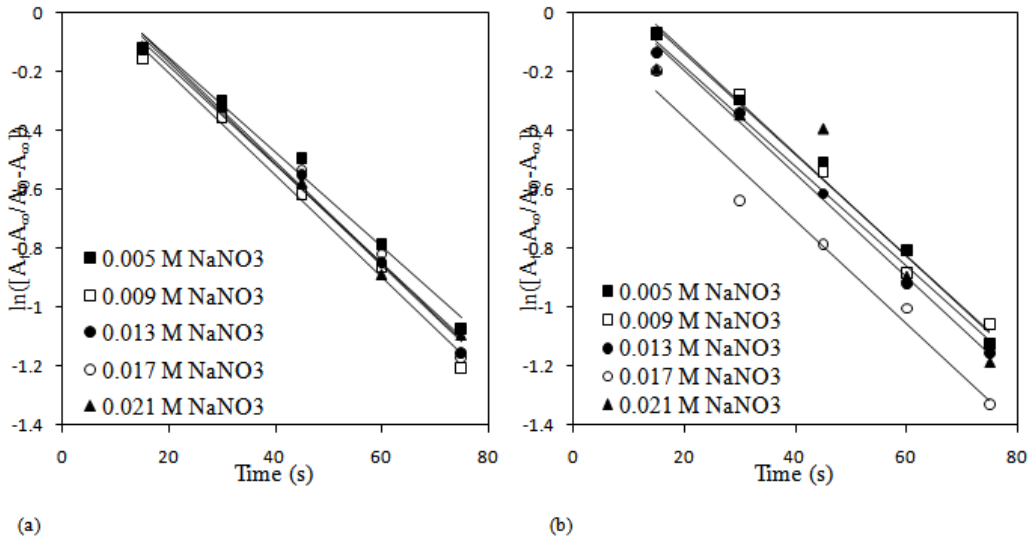

Figure 10: Effects of dissolved organic matter, DOM obtained from (a) saw dust and (b) maize cob on the rates of reaction of AsO_2^- with $Cr_2O_7^{2-}$ at varying ionic strengths (molL^{-1}).

Table 5: Pseudo-first order, k_I data for the oxidation-reduction reaction between AsO_2^- and $Cr_2O_7^{2-}$ ions and in the presence of dissolved organic matter, DOM from saw dust and maiz cob at varying ionic strength (0.005 – 0.021 molL^{-1} $NaNO_3$).

I (molL^{-1})	$k_I(s^{-1})$ $AsO_2^-/Cr_2O_7^{2-}$	$k_I(s^{-1})$ for $AsO_2^-/Cr_2O_7^{2-}$/DOM	
		Saw dust	Maize cob
0.005	0.015	0.016	0.017
0.009	0.015	0.017	0.017
0.013	0.016	0.017	0.017
0.017	0.017	0.017	0.017
0.021	0.018	0.016	0.016

3.8 Effect of Temperature on the Reaction Rate

The results of temperature dependence studies for the oxidation-reduction reaction between AsO_2^- and $Cr_2O_7^{2-}$ ions, and in the presence of DOM showed that as the temperature increased, the reaction rates increased,

Figure 11, have plots of these reactions; $AsO_2^-/Cr_2O_7^{2-}$/DOM(SD) and $AsO_2^-/Cr_2O_7^{2-}$/DOM(MC) and Table 6 have values of the above reactions. The values of activation energy (E_a), enthalpy change, ΔH and entropy change, ΔS were calculated from Arrhenius and Eyring's plots respectively and are presented in Table 7. A high E_a value signifies that the rate constant depends strongly on temperature [30], and that a slow reaction would have a higher energy of activation [36]. In our studies, it is evident the higher Ea value for the oxidation-reduction reaction between AsO_2^- and $Cr_2O_7^{2-}$ ions in the absence of DOM (Ea = 52.01 kJmol^{-1}, Table 7) with a lower k_{obs} value (0.006 s^{-1} at 288 K, Table 6) than in the presence of DOM (48.22 kJmol^{-1} and 46.46 kJmol^{-1} for DOM from saw dust and maize cob, Table 7) with higher k_{obs} values (0.008 s^{-1} and 0.008 s^{-1} at 288 K for DOM from saw dust and maize cob), Table 6). The negative ΔH values of these reactions are indicative of the exothermic nature of the oxidation-reduction reactions considered which conforms to the low temperature requirement of these reactions in nature [37]. The values of enthalpy and entropy of activation together give us free energy, ΔG for the reactions considered in the range (-0.4676 kJmol^{-1}) at 308 K – (-16.4431 kJmol^{-1}) at 288 K, the values are indicative of the spontaneity of these AsO_2^- and $Cr_2O_7^{2-}$ oxidation-reduction reactions [16, 37].

Furthermore, the oxidation-reduction reaction between AsO_2^- and $Cr_2O_7^{2-}$ ions in the presence of DOM from saw dust and DOM from maize cob were considered at 0 ^oC (273 K), (Figure 12) contains plots for $AsO_2^-/Cr_2O_7^{2-}$/DOM reactions and Table 6 has values of the reactions. The results showed an increased reaction rates in both cases at this temperature or the reactions rates were comparable to the rate of these reactions at say 30 ^oC (303 K) – 35 ^oC (308 K), the increased reactions rates at this temperature compared to aqueous phase (or other temperatures) could likely be due to the freeze concentration effect [7]. The concentrations of DOM, protons and $Cr_2O_7^{2-}$ were highly concentrated in the ice grain boundary region, which accelerated the reaction rates. Similar effect was noticed by Xiaoling, D. et al, 2014. Thus, concentrating either protons or DOM in the aqueous phase had a similar effect as in the ice phase.

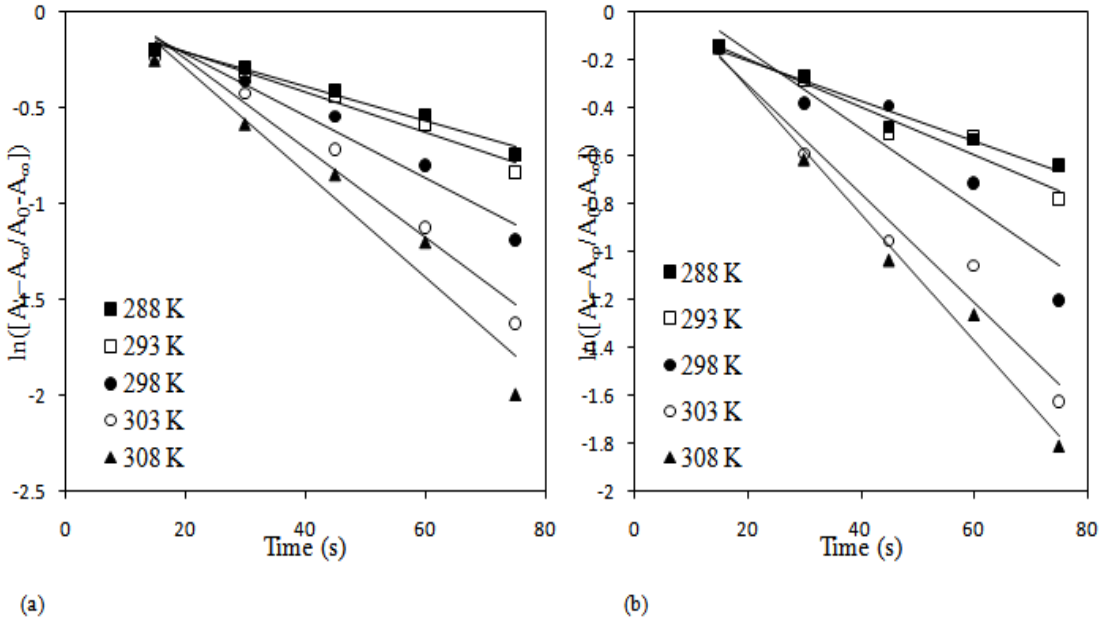

Figure 11: Effects of temperature (K) variation on the rates of reaction between AsO_2^- and $Cr_2O_7^{2-}$ in the presence of dissolved organic matter, DOM obtained from (a) saw dust and (b) maize cob.

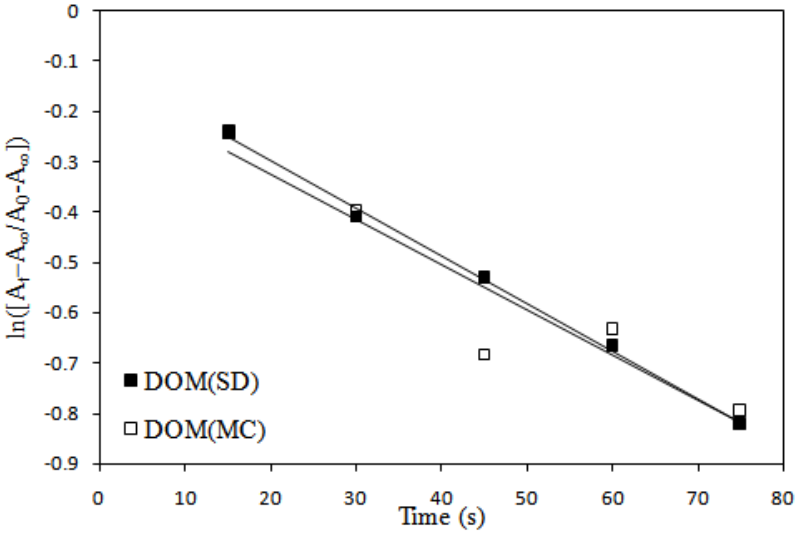

Figure 11: Effects of dissolved organic matter, DOM (SD = saw dust, MC = maize cob) on the rates of redox reaction between AsO_2^- and $Cr_2O_7^{2-}$ at 273 K.

Table 6: Pseudo-first order, k_T data for the oxidation-reduction reaction between AsO_2^- and $Cr_2O_7^{2-}$ ions and in the presence of dissolved organic matter, DOM from saw dust and maize cob at varying temperatures (273, 288 – 308 K).

T (K)	k_T(s^{-1}) for $AsO_2^-/Cr_2O_7^{2-}$	k_T (s^{-1}) for $AsO_2^-/Cr_2O_7^{2-}$/DOM	
		Saw dust	Maize cob
273	-	0.009	0.009
288	0.006	0.008	0.008
293	0.008	0.010	0.010
298	0.015	0.016	0.016
303	0.020	0.023	0.022
308	0.022	0.027	0.026

Table 7: Activation parameters (activation energy, enthalpy change and entropy change) of the oxidation-reduction reactions; $AsO_2^-/Cr_2O_7^{2-}$ and $AsO_2^-/Cr_2O_7^{2-}$/DOM.

Nature of Reaction	Activation Energy, Ea KJmol^{-1}	Enthalpy Change, ΔH KJmol^{-1}	Entropy Change, ΔS Jmol^{-1}K^{-1}
$AsO_2^-/Cr_2O_7^{2-}$	52.01	-49.54	-114.92
$AsO_2^-/Cr_2O_7^{2-}$/DOM(SD)	48.22	-45.74	-126.15
$AsO_2^-/Cr_2O_7^{2-}$/DOM(MC)	46.46	-43.98	-132.20

Key;
DOM(SD) = DOM from saw dust
DOM(MC) = DOM fro maize cob

IV. Conclusion

The simultaneous oxidation of arsenic(III) and reduction of chromium(VI) in aqueous phase in the presence of dissolved organic matter, DOM is reported and from this study, the metal ions evidently changed in their oxidation states. The reactions are first order in both AsO_2^- and $Cr_2O_7^{2-}$ and second order overall. The k_{obs} values are higher for $Cr_2O_7^{2-}$ than for AsO_2^- and are affected by DOM. The reaction rates are relatively higher for the agro-wastes-DOM obtained from saw dust than for maize cob and the rates of the reactions at 273 K are relatively high and comparable to the reactions at 303 – 308 K.

Acknowledgements

We appreciate Tertiary Education Trust Fund (TETFund) Nigeria for given us research grant. Our appreciation also goes to the Department of Chemistry, Benue State University, Makurdi-Nigeria for given us access to their laboratory.

References

[1]. C. R. Ramakrishnaiah and B. Prathima, Hexavalent chromium removal from industrial watsewater by chemical precipitation method, International Journal of Engineering Research and Applications (IJERA), 2012, 2(**2**); 599-603.

[2]. J. H. Duffus, Heavy metals-a meaningless term? International Union of Pure and applied Chemistry, 2002, 74(**5**); 793–807.

[3]. A. Arruti, I. Fernández-Olmo and A. Irabien, Evaluation of the contribution of local sources to trace metals levels in urban PM2.5 and PM10 in the Cantabria region (Northern Spain), Journal of environmental monitoring, 2010, 12(**7**); 1451–1458.

[4]. G. Dönmez and Z. Aksu, Removal of chromium (VI) from saline wastewaters by Dunaliella species, Research Journal of Environmental Toxicology, 2002, 38(**5**); 751–762.

[5]. J. A. Wilkie, and J. G. Hering, Rapid oxidation of geothermal arsenic(III) in stream waters of the Eastern Sierra Nevada, Environmental science and technology, 1998, 32; 657–662.

[6]. V. Charalampos, M. Ifigenia, M. Ecconomou-Eliopoulos and M. Loannis, "Hexavalent chromium and other toxic elements in natural waters in the Thiva – Tanagra – Malakasa Basin, Greece". Hellenic Journal of Geosciences. 2008, 43; 57–56.

[7]. D. Xiaoling, Q. Lena, J. G. Mab, H. Willie and L. Yuncong, Enhanced Cr(VI) reduction and As(III) oxidation in ice phase: Important role of dissolved organic matter from biochar, Journal of Hazardous Materials, 2014, 267; 62– 70.

[8]. B. T. Iorhuna, R. A. Wuana and S. G. Yiase. (2020). Simultaneous Studies of Redox Reaction of Chromium(VI) and Arsenic(III) in Aqueous Phase: A Kinetic and Mechanistic Approach, Asian Journal of Chemical Sciences, 7(2): 18 - 29,

[9]. A. S. Shaaban, M. M. Nona-Marry and M. F. Dimin, Characterization of biochar derived from rubber wood sawdust through slow pyrolysis on surface porocities and functional groups, International Tribology conference, Malaysia, 2013, 68; 365-371.

[10]. C. A. Black, (ed.), Methods of Soil Analysis; Agronomy, No.9, Part 2 American Society of Agronomy, Madison, Wisconsin, 1965.

[11]. A. Walkley and I. A. Black, An Examination of the Degtjareff Method for Determining Soil Organic Matter and Proposed Modification of the Chromic Acid Titration Method, Soil Sciences, 1934, 37: 29-38.

[12]. L. Man Kee and Z. Ridzuan, Production of activated carbon from sawdust using fluidized bed reactor, International Conference on Environment, (ICENV 2008)

[13]. K. Hammes, R. J. Smernik, J. O. Skjemstad and M. W. Schmidt, "Characterisation and evaluation of reference materials for black carbon analysis using elemental composition, colour, BET surface area and ^{13}C NMR spectroscopy," Applied Geochemistry, 2008, 23(**8**); 2113–2122.

[14]. R. M. Verma, Analytical chemistry, theory and practice. CBS publishers and distributors PVT Ltd, India, 2010, 358-61.

[15]. H. K. Amira, F. E. Samah and F. H. Sherin, A review on UV spectrophotometric methods for simultaneous multicomponent analysis, European Journal of Pharmaceutical and Medical Research, 2016, 3(2); 348-360

[16]. B. Dionisio, G. Diego, L. P. Jaqueline, R. O. Juliane, G. A. Karina and L. C. Rodolfo, Kinetic and thermodynamic parameters of biodiesel oxidation with synthetic antioxidants: simplex centroid mixture design, Journal of Brazilian Chemical Society, 2014, 25(**11**); 32-40.

[17]. L. K. Ong, A. Kurniawan, A. C. Suwandi, C. X. Lin, X. S. Zhao and S. Ismadji,Transesterification of leather tanning waste to biodiesel at supercritical condition: Kinetics and thermodynamics studies, The Journal of Supercritical Fluids, 2013, 75; 11–20.

[18]. C. Cheong-Song, K. Jin-Woo, J. Cheol-Jin, K. Huiyong and Y. Ki-Pung, Transesterification kinetics of palm olein oil using supercritical methanol, The Journal of Supercritical Fluids, 2011, 58(**3**); 365–370.

[19]. S. O. Adejo, S. G. Yiase, P. O. Ukoha, B. T. Iorhuna and J. A. Gbertyo, U.Oxidation-reduction reaction of chromium(VI) and iron(III) with paracetamol: kinetics and mechanistic studies, Archives of Applied Science Research, 2014, 6(**5**); 56-67.

[20]. A. A. Helal, G. A. Murad and A. A. Helal, Characterization of different humic materials by various analytical techniques, Arabian Journal of Chemistry, 2011, 4(**1**); 51-54

[21]. G. Shie-Jie, Z. Chen, S. Zong-Hai, Z. Jun, L. Jian-Guo and L. Jun-Qing, Spectroscopic Characteristics of Dissolved Organic Matter in Afforestation Forest Soil of Miyun District, Beijing, Journal of Analytical Methods in Chemistry, 2016, 5; 56-62.

[22]. R. M. Silverstein, F. X. Webster and D. J. Kiemle, Spectrometric Identification of organic compounds, 7th ed. John Wiley and Sons International, 2005, Pp.72-126.

[23]. K. Shamshad, Y. Wu, X. Zhang, J. Liu, J. Sun and S. Hu, Estimation of Concentration of Dissolved Organic Matter from Sediment by using UV–Visible Spectrophotometer, International Journal of Environmental Pollution and Remediation, 2014, 2(**1**); 24-29.

[24]. P. L. Smedley and D. G. Kinniburg, A review of the source, behavior and distribution of arsenic in natural waters, Applied Geochemistry, 2002, 17; 517-568.

[25]. D. G. Brookins, Eh-pH diagrams for geochemistry. Springer-Verlag, Berlin, Germany.

[26]. P. Atkins and J. De paula, Physical Chemistry, 7th ed. Oxford University Press. New Delhi, 2000, Pp 960-62.

[27]. M. Ajmal, A. A. Nomani and A. Ahmad, Acute toxicity of chrome electroplating wastes to microorganisms: adsorption of chromate and chromium(VI) on a mixture of clay and sand, Water, Air, and Soil Pollution, 1984, 23(**2**); 119–127.

[28]. D. C. Schroeder and G. F. Lee, Potential transformation of chromium in natural waters, Water, Air, and Soil Pollution, 1975, 4; 355–365.

[29]. A. U. Israel, I. B. Obot, S. A. Umoren, V. Mkpenie and J. E. Asuquo, Production of Cellulosic Polymers from Agricultural Wastes, E-Journal of Chemistry, 2008, 5(1); 81-85.

[30]. F. A. Cotton and G. Wilkison, Advanced Inorganic Chemistry; A Comprehensive Text. 3rd ed. Wiley Eastern Ltd, New Delhi, 1978, Pp 818-870.

[31]. J. M. Pacyna and E. G. Pacyna, An assessment of global and regional emissions of trace metals to the atmosphere from anthropogenic sources worldwide, Environmental Review, 2001, 9(4); 269-298.

[32]. K. Martina and P. Miloslav, Solubility and dissociation of lignitic humic acids in water suspension, Colloids and Surfaces A: Physicochemical and Engineering Aspects, 2005, 252(2-3); 157-163

[33]. H. Kipton, J. Powell and R. M. Town, Solubility and fractionation of humic acid; effect of pH and ionic medium, Analytica Chimica Acta, 1992, 267(**1**); 47-54

[34]. P. Kumar, Study of effect of variation of ionic strength of the medium on velocity constant of Ru(III) catalyzed oxidation of hydroxyl benzoic acids by chloramine-T in acidic medium, oriental Journal of Chemistry, 2013, 29(**4**);23-28.

[35]. N. C. Hughes-Jones, B. Gardner and R. Telford, The Effect of pH and Ionic Strength on the Reaction between Anti-D and Erythrocytes, Immunology, 1964, 7; 72-81.

[36]. Y. Cantu, A. Remes, A. Reyna, D. Martinez, J. Villarreal, H. Ramos, S. Trevino, C. Tamez, E. T. Martinez and J. G. Parsons, Thermodynamics, Kinetics, and Activation energy Studies of the sorption of chromium(III) and chromium(VI) to a Mn_3O_4 nanomaterial, Chemical Engineering Journal, 2014, 254(15); 374-383.

[37]. A. A. Attia, S. A. Khedr and S. A. Elkholy, Adsorption of chromium(VI) ion by acid activated carbon, Brazilian Journal of Chemical Engineering, 2010, 27(**1**); 45-59.